

## Electronic Supplementary Information

### Mixed AgBiS<sub>2</sub> nanocrystals for photovoltaics and photodetectors

Ignasi Burgués-Ceballos,<sup>1</sup> Yongjie Wang,<sup>1</sup> and Gerasimos Konstantatos<sup>1,2</sup>

1. ICFO-Institut de Ciències Fotòniques, The Barcelona Institute of Science and Technology, 08860 Castelldefels (Barcelona), Spain

2. ICREA-Institució Catalana de Recerca i Estudis Avançats, Passeig Lluís Companys 23, 08010 Barcelona, Spain

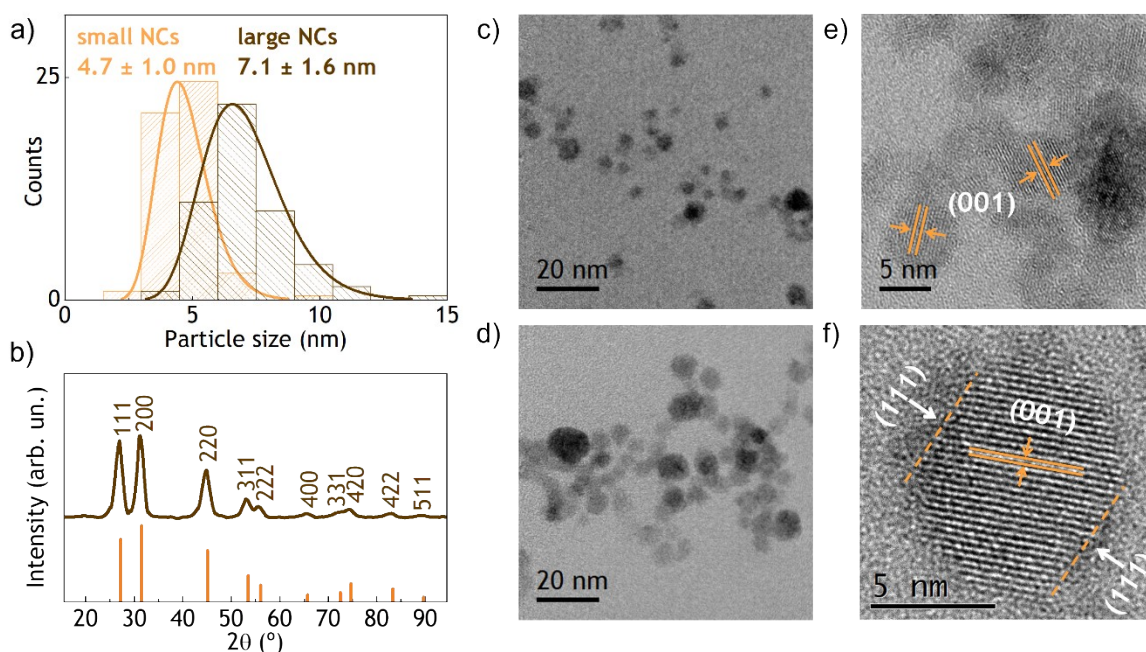


**Figure S1** Characterisation of AgBiS<sub>2</sub> nanocrystals. a) Particle size distribution of the two synthetic batches, determined from TEM analyses. b) X-ray diffraction pattern of the larger nanocrystals showing a good correlation with the reference pattern of cubic AgBiS<sub>2</sub>. TEM micrographs of c) small-size and d) large-size AgBiS<sub>2</sub> nanocrystals. High-resolution TEM (HRTEM) micrographs of e) small-size and f) large-size NCs showing only the (001) non-polar facet. The two cuts on the cubic nanocrystal along the (111) direction are highlighted in the large NC.

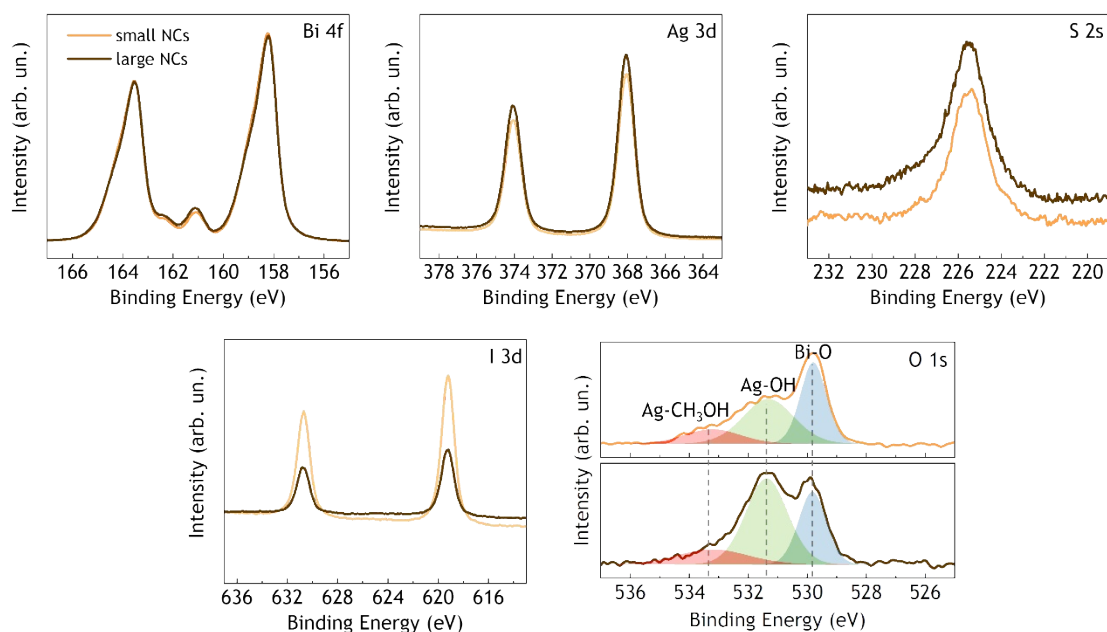


**Figure S2** XPS core-level spectra of small and large nanocrystals. In the O 1s spectra, the shaded areas represent the fitted components.

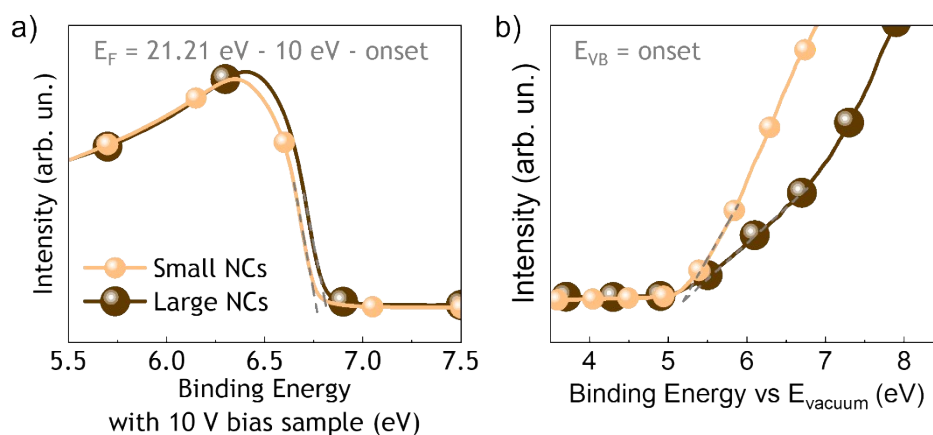


**Figure S3** a) High binding energies of secondary electron cut-off for Fermi level calculation while 10 V bias was applied. b) Low binding energies of secondary electron cut-off, corrected to Fermi level position, for valence band calculation.

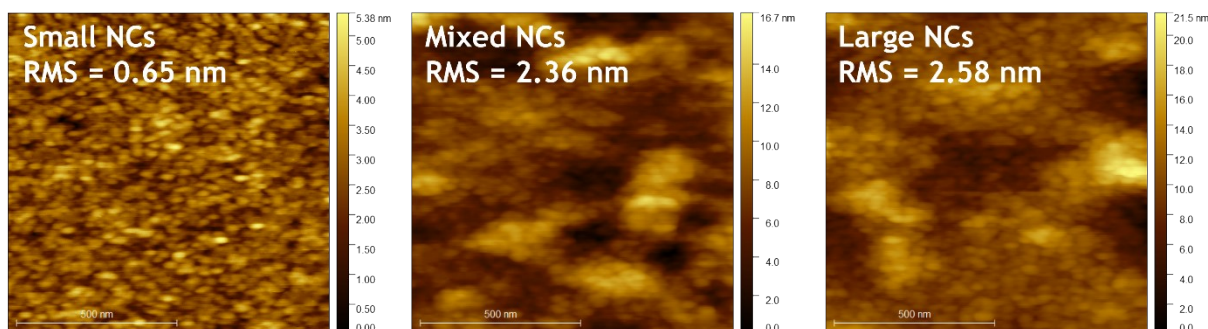


**Figure S4** Atomic force microscopy images of  $\text{AgBiS}_2$  layers using small, mixed and large nanocrystals.

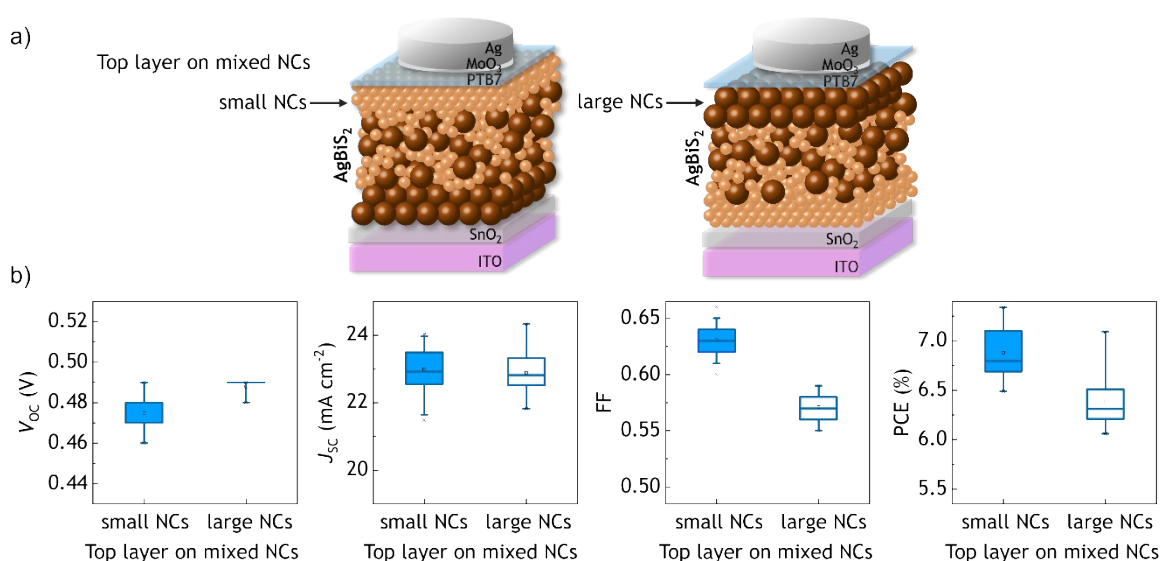


**Figure S5** a) Schematic cross-section of photoactive devices using the gradient fashion architecture with small (left drawing, favourable gradient) or large (right drawing, unfavourable gradient)  $\text{AgBiS}_2$  nanocrystals on top of the mixed NCs layer(s). b) Statistical data of the main photovoltaic performance parameters, comparing the two device architectures described in a).

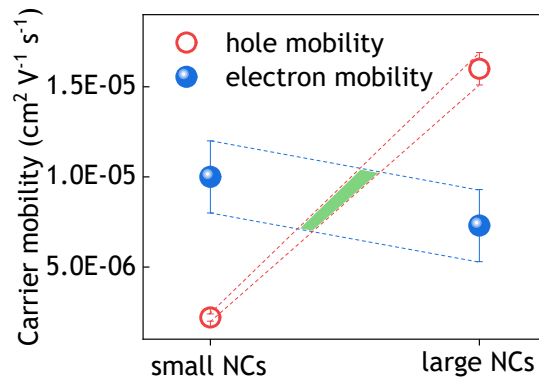


**Figure S6** Charge carrier mobility of the small and large NCs extracted from space-charge-limited current measurements, as reported elsewhere.<sup>1</sup> The shaded area indicates the region where the effective hole:electron mobility balance is closest to 1, which corresponds to the 1:1 mixture of NCs.

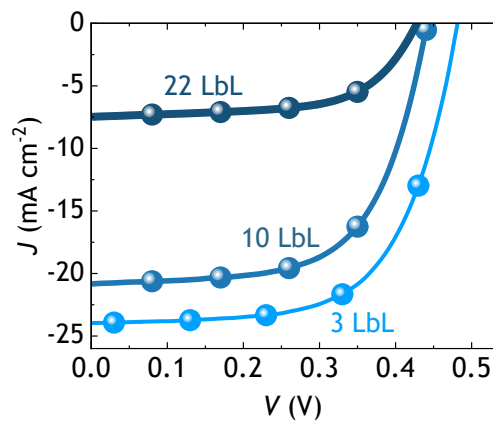


**Figure S7** *JV* characteristics under 1 sun of devices using mixed NCs with different active layer thicknesses: ~35 nm (3 LbL), ~140 nm (10 LbL), and ~260 nm (22 LbL)

## Experimental Section

### Materials

All the reagents were purchased from Sigma Aldrich, except for Bi(OAc)<sub>3</sub> and SnO<sub>2</sub> precursor (tin(IV) oxide, 15% in H<sub>2</sub>O colloidal dispersion), which were obtained from Alfa Aesar. Poly[[4,8-bis[(2-ethylhexyl)oxy]benzo[1,2-b:4,5-b']dithiophene-2,6-diyl][3-fluoro-2-[(2-ethylhexyl)carbonyl]thieno[3,4-b]thiophenediyl]] (PTB7) was

purchased from 1-Material. The ITO-covered glass substrates were acquired from the Institut für Großflächige Mikroelektronik, Universität Stuttgart.

### **Synthesis of AgBiS<sub>2</sub> nanocrystals**

All the reactions were carried out using standard Schlenk techniques. To obtain the small-sized nanocrystals, we followed our previously reported, low-temperature hot-injection synthetic route.<sup>2</sup> In brief, 1 mmol Bi(OAc)<sub>3</sub>, 0.8 mmol Ag(OAc) and 17 mmol oleic acid (OA) were pumped overnight at 100 °C to form the Bi and Ag oleates and remove oxygen and moisture. After that, the reaction atmosphere was switched to Ar, to quickly inject 1 mmol hexamethyldisilathiane (HMS) dissolved in 5 ml 1-octadecene (ODE) under vigorous stirring. The heating was stopped, without removing the heating mantle, and the reaction was allowed to cool down slowly. Upon addition of acetone and centrifugation, the nanocrystals were isolated and purified by successive dispersion in toluene and precipitation with acetone. The oleic-capped colloidal nanocrystals were finally dispersed in anhydrous toluene and 0.45 µm polytetrafluoroethylene (PTFE) filtered. To obtain the larger-sized NCs, we modified slightly our previously reported double-step hot-injection synthesis.<sup>1</sup> While the stoichiometric amounts were identical as in the single-step synthesis, the addition of the sulphur precursor was done in two steps: first, 0.1 mmol HMS were quickly injected. After 2 min and without removing the heating, the remaining 0.9 mmol HMS were added dropwise at a rate of 0.35 mL min<sup>-1</sup>. The heating was removed once all the sulphur precursor was added.

### **Characterisation of AgBiS<sub>2</sub> nanocrystals**

TEM measurements were performed at the Scientific and Technological Centres of the University of Barcelona (CCiT-UB). TEM micrographs were obtained using a JEOL 2100 microscope operating at an accelerating voltage of 200 kV. The samples were

prepared by placing one drop of a diluted toluene solution on a holey carbon-coated grid and allowing the solvent to evaporate in air. The average diameter was calculated by measuring the diameters of  $\sim 100$  nanocrystals from non-aggregated areas. X-ray diffraction spectra were obtained using a Rigaku SmartLab II powder diffractometer with Cu K $\alpha$  radiation ( $\lambda = 1.5406\text{\AA}$ , 45 kV, 40 mA). The samples were prepared by dropcasting a concentrated dispersion of AgBiS<sub>2</sub> nanocrystals onto glass slides. X-ray photoelectron spectroscopy (XPS) and ultraviolet photoelectron spectroscopy (UPS) measurements were performed at the Institut Català de Nanociència i Nanotecnologia (ICN2) with a Specs Phoibos 150 analyser in ultra-high vacuum conditions (base pressure of  $10^{-10}$  mbar) using a monochromatic HeI radiation (21.2 eV) for UPS and a monochromatic K $\alpha$  X-ray source (1486.74 eV) for XPS. Accurate binding energies (0.2 eV) were determined by referencing to the C 1s peak at 284.8 eV. The samples were prepared by covering ITO substrates ( $\sim 10 \times 10 \text{ mm}^2$ ) with concentrated AgBiS<sub>2</sub> toluene-based solutions and allowing the solvent to evaporate in air.

### **Fabrication of solar cells and photodetectors**

ITO-covered glass substrates were cleaned by sequential ultrasonication in soapy water, acetone and isopropanol for 10 min each and dried with nitrogen. As the electron transport, a  $\sim 30$  nm SnO<sub>2</sub> layer was coated on top of ITO by spin casting at 2000 rpm a water-based colloidal dispersion (Alfa Aesar SnO<sub>2</sub> colloid solution diluted 1 to 5.6 v/v in H<sub>2</sub>O) and annealed in air at 275 °C for 30 min. Then, a layer-by-layer (LbL) process was followed to deposit the AgBiS<sub>2</sub> films. Each LbL step consisted of i) casting one drop of 20 mg ml<sup>-1</sup> solution of AgBiS<sub>2</sub> in toluene onto the SnO<sub>2</sub> at a spinning speed of 2000 rpm and waiting 10 s, ii) adding 5 drops of tetramethylammonium iodide (TMAI, 1 mg ml<sup>-1</sup> in methanol) and waiting 20 s, iii) repeating step ii, iv) rinsing with methanol and then with toluene. In all the devices, the first (last) AgBiS<sub>2</sub> layer consisted of only large (small) NCs. The inner layers contained a mixture of the two

batches with a ratio of 1:1. To modify the thickness of the absorbing layer, the number of those intermediate LbL steps was changed from 1 to 20. For the record solar cell devices the optimum thickness was set to ~35 nm, corresponding to a total of 3 LbL. The best performing photodetectors, instead, had a total of 20 LbL; the thicknesses of the films are given as approximate from a calibration (thickness measured with a profilometer) related to the number of layers deposited. After the deposition of AgBiS<sub>2</sub>, the samples were annealed for 10 min at 100 °C in air and then stored in the dark overnight. Then, a thin (~6 nm) layer of PTB7 was spin cast at 2000 rpm from a 5 mg ml<sup>-1</sup> solution in o-Dichlorobenzene. Finally, 3 nm of MoO<sub>3</sub> and 150 nm of Ag were sequentially evaporated through a shadow mask (2 mm diameter, 3.1 mm<sup>2</sup> area) in a Kurt J. Lesker Nano36 system.

### **Characterisation of solar cells and photodetectors**

The current–voltage measurements were performed with a Keithley 2400 source meter and a calibrated Newport Oriel Sol3A solar simulator (AM 1.5 G) under ambient conditions. The EQE spectra were measured using a Newport Cornerstone 260 monochromator, a Thorlabs MC2000 chopper, a Stanford Research SR570 trans-impedance amplifier and a Stanford Research SR830 lock-in amplifier. A calibrated Newport 818-UV photodetector was used as a reference.

### **References**

- (1) Burgués-Ceballos, I.; Wang, Y.; Akgul, M. Z.; Konstantatos, G. Colloidal AgBiS<sub>2</sub> Nanocrystals with Reduced Recombination Yield 6.4% Power Conversion Efficiency in Solution-Processed Solar Cells. *Nano Energy* **2020**, *75*. <https://doi.org/10.1016/j.nanoen.2020.104961>.
- (2) Bernechea, M.; Miller, N. C.; Xercavins, G.; So, D.; Stavrinadis, A.; Konstantatos, G. Solution-Processed Solar Cells Based on Environmentally Friendly AgBiS<sub>2</sub> Nanocrystals. *Nat. Photonics* **2016**, *10* (8), 521–525. <https://doi.org/10.1038/nphoton.2016.108>.